JOURNAL OF MATERIALS SCIENCE **35** (2000) 5563–5567

X-ray diffraction study of compositionally homogeneous, nanocrystalline yttria-doped zirconia powders

D. G. LAMAS*, N. E. WALSÖE DE RECA
PRINSO (Programa de Investigaciones en Sólidos), CITEFA-CONICET, Zufriategui 4380, (1603) Villa Martelli, Pcia. de Buenos Aires, Argentina
E-mail: lamasd@cab.cnea.gov.ar

The crystal structure of compositionally homogeneous, nanocrystalline ZrO_2 - X mol% Y_2O_3 ($X = 2.8$, 4, 5, 6, 7, 8, 9, 10, 11, and 12) powders synthesized by a nitrate-citrate gel-combustion process has been studied by X-ray diffraction. By applying the Rietveld method, it was found that all the powders presented the tetragonal phase ($P4_2/nmc$ space group). The axial ratio c/a_f decreased with increasing Y_2O_3 content and became almost unity at 9 mol% Y_2O_3. However, powders in the compositional range of ZrO_2 - 9 to 12 mol% Y_2O_3 exhibited the oxygen atoms displaced from their ideal sites of the cubic phase along the *c* axis, which is known as the t″-form of the tetragonal phase. A conjunct analysis of crystallite size and microstrain of all the powders is also presented.

1. Introduction

Zirconia-based ceramics are widely studied because of their excellent electrical and mechanical properties. They are applied in electrochemical cells (fuel cells, oxygen sensors, oxygen pumps, etc.) due to their high oxide-ion conductivity at elevated temperatures [1, 2]. Furthermore, they are tough, wear resistant and show a low heat conductivity, so these materials are useful from the structural point of view [3, 4].

One of the most notable characteristics of some compositionally homogeneous zirconia-based solid solutions is the existence of three tetragonal forms, all belonging to the $P4_2/nmc$ space group [5–14]. The stable tetragonal form is called the t-form, which is restricted to the solubility limit predicted by the equilibrium phase diagram. There is also a t′-form with an expanded solubility but unstable in comparison with the mixture of the t-form and cubic phase. Finally, the t″-form has an axial ratio c/a_f of unity but with the oxygen atoms displaced along the *c* axis from their ideal sites of the fluorite-type cubic phase (8c sites of the Fm $\bar{3}$ m space group). Table I summarizes these definitions.

The t′/t″ and t″/c boundaries have been investigated by Yashima *et al*. in several systems, such as ZrO_2-Y_2O_3 [5–8], ZrO_2-Er_2O_3 [7–10], ZrO_2-Nd_2O_3 [8], ZrO_2-Sm_2O_3 [8], ZrO_2-Yb_2O_3 [8], ZrO_2-CeO_2 [11–13] and ZrO_2-CaO [14]. For the ZrO_2-Y_2O_3 system, these authors have carefully characterized compositionally homogeneous powders synthesized by arc melting and rapid quenching [5, 7, 8] or by the solid-state reaction method [6]. They found that the t′/t″ and t″/c boundaries were located around 9 and 11 mol% Y_2O_3, respectively.

In a recent work [15], we have investigated the crystal structure of compositionally homogenous, nanocrystalline ZrO_2 - 12 mol% Y_2O_3 powders synthesized by a nitrate- citrate gel-combustion process. We found that these powders presented the t″-form of the tetragonal phase, while the assumption of the fluorite structure gave lower agreement factors. These results were in disagreement with the above-mentioned works of Yashima *et al*. [5–8], since they reported that powders with Y_2O_3 content higher than 11 mol% exhibited the cubic phase. We also found that the oxygen ion displacement decreased with increasing crystallite size.

The aim of this work is the study of the tetragonal forms present in compositionally homogeneous, nanocrystalline ZrO_2 - 2.8 to 12 mol% Y_2O_3 powders prepared by the same gel-combustion process. Gel-combustion synthesis produces highly reactive, compositionally homogeneous powders, as has been demonstrated by several authors [16–19]. The crystallographic analysis was performed by X-ray diffraction applying the Rietveld method. By employing this method, it was possible to identify the tetragonal forms by refining the cell parameters and the fractional *z*-coordinate of the oxygen ion in the tetragonal asymmetric unit.

2. Experimental procedure

2.1. Powder synthesis

Compositionally homogeneous, nanocrystalline ZrO_2 - X mol% Y_2O_3 ($X = 2.8$, 4, 5, 6, 7, 8, 9, 10, 11, and 12)

* *Present address*: Sección Caracterización de Materiales, Centro Atómico Bariloche (CAB), CNEA. Av. E. Bustillo km 9.5, (8400) S.C. de Bariloche, Pcia. de Río Negro, Argentina.

TABLE I Classification of the tetragonal forms and the cubic phase

Form	Space group	System	Oxygen displacement	Axial ratio (c/a_f)
t	$P4_2/nmc$	Tetragonal	Yes	>1
t′	$P4_2/nmc$	Tetragonal	Yes	>1
t″	$P4_2/nmc$	Tetragonal	Yes	=1
c	$Fm3m$	Cubic	No	=1

powders were synthesized by a nitrate-citrate gel-combustion process already reported by the authors [20, 21]. Zirconium oxychloride (Merck) and yttrium oxide (Riedel-de Haën) were dissolved in an excess of nitric acid in a ratio corresponding to the desired final composition and this nitrate solution was concentrated to a low volume by thermal evaporation in order to eliminate chlorine. Citric acid in a proportion of 2 moles per mole of metal atom was added and the pH of the solution was adjusted to pH = 7 with ammonium hydroxide. The resulting solution was then concentrated on a hot plate (at 200–300°C) until a black gel was obtained, which finally burned due to a vigorous exothermic reaction between nitrate and citrate ions. The resulting gray ashes were treated at 350°C in air for an hour to eliminate the carbonaceous residues and then calcined at 600°C for two hours. The system was homogeneous during the whole process and no precipitation was observed. All the chemicals used for this synthesis were of analytical reagent grade.

2.2. Structural characterization

The as-synthesized powders were studied by X-ray diffraction (XRD) employing a PW 3710 Philips diffractometer operated at 40 kV and 30 mA with Cu-K_α radiation and a graphite monochromator. Data in the angular region of $2\theta = 20$–90° were collected in a step-scanning mode, with a step length of 0.02°.

The structural study was performed by the Rietveld analysis program FullProf [22]. The $P4_2/nmc$ space group was assumed with (Zr^{4+}, Y^{3+}) cations and O^{2-} anions in 2a and 4d positions, respectively. The cell parameters, a and c, and the fractional z coordinate of the O^{2-} anion in the tetragonal asymmetric unit, z(O), were refined. A tetragonal unit cell was used instead of the usual pseudo-fluorite one. However, the axial ratio c/a_f ($a_f = \sqrt{2}a$) will be referred to the pseudo-fluorite cell (See ref. [15] for details of both choices). In order to carry out a conjunct study of crystallite size and microstrain, the peak shape was assumed to be a modified Thompson-Cox-Hasting pseudo-Voigt (TCHZ-pV) function [23]. The background of each profile was adjusted by a six-parameter polynomial function in $(2\theta)^n$, $n = 0$–5. Isotropic atomic thermal parameters were used.

For powders with a composition of ZrO_2 - 12 mol% Y_2O_3, the above $P4_2/nmc$ structural model was compared with the fluorite one: $Fm3m$ space group with (Zr^{4+}, Y^{3+}) cations and O^{2-} anions in 4a and 8c positions, respectively.

Data in the angular region of $2\theta = 70$–77° were carefully collected in order to observe the splitting of $(400)_f$ and $(004)_f$ reflections in case of the presence of t or t′ forms, while the t″ form and the cubic phase only present one line. As above, the subscript f indicates that these lines are referred to the pseudo-fluorite cell.

3. Results and discussion

The proposed nitrate-citrate gel-combustion route is based on the exothermic reaction between nitrate and citrate ions present in the precursor gel. The large volume of gases produced during this reaction promotes the disintegration of the precursor giving nanocrystalline particles. A detailed study of this process has been reported by the authors in a recent paper [21], showing the complete retention of the metastable tetragonal phase in the case of ZrO_2 - 2.8 mol% Y_2O_3 powders. A mean crystallite size of about 10 nm was obtained.

A qualitative analysis of the diffractograms (Fig. 1) showed that all the powders exhibited the metastable tetragonal and/or cubic phases. In spite of being stable at room temperature for concentrations of Y_2O_3 lower than 8–9 mol% (according to the equilibrium phase diagram proposed by Scott [24]), the monoclinic phase was not found in any sample. Fig. 2 shows the high-angle region of the diffractograms, which can be used for distinguishing the t and t′ forms (which present the splitting of $(400)_f$ and $(004)_f$ lines in this region) from the t″ form or cubic phase. For powders with Y_2O_3 content lower than 5 mol% the $(400)_f$ and $(004)_f$ lines could be resolved, while those with Y_2O_3 content than 9 mol% presented one line. For intermediate compositions it was not possible to discriminate between these two cases because of line broadening.

For an estimation of the crystallite size, the Scherrer equation [25] was employed:

$$D = \frac{0.9\lambda}{\beta \cos\theta} \tag{1}$$

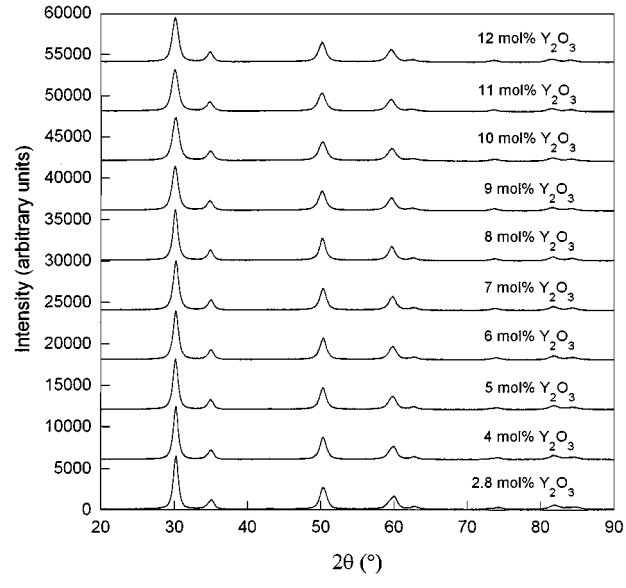

Figure 1 Diffractograms of the nanocrystalline ZrO_2 - 2.8 to 12 mol% Y_2O_3 powders.

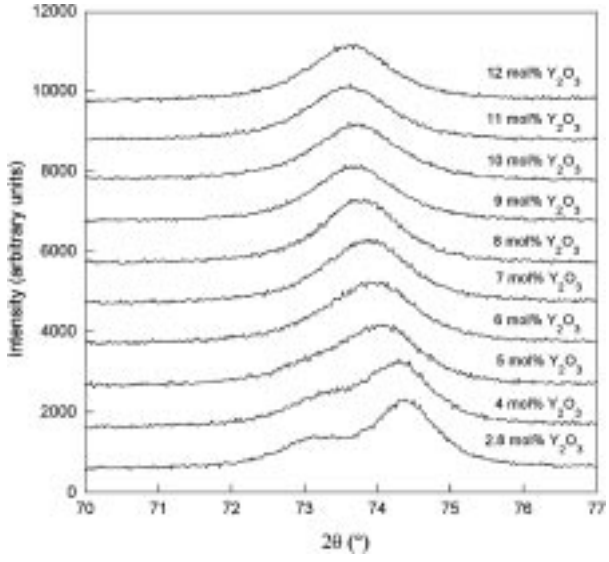

Figure 2 High-angle region of the diffractograms of the ZrO_2 - 2.8 to 12 mol% Y_2O_3 powders. The t and t′-forms exhibit the splitting of $(400)_f$ and $(004)_f$ reflections, while the t″-form presents only one line, as in the case of the cubic phase.

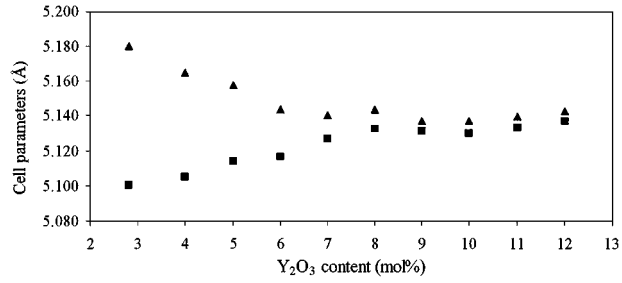

Figure 3 Variation of the structural parameters a_f and c (referred to the pseudo-fluorite cell) with the Y_2O_3 content.

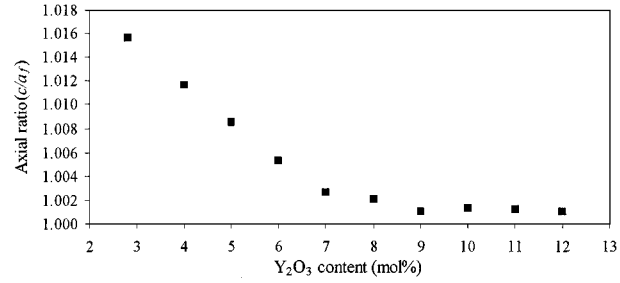

Figure 4 Variation of the axial ratio c/a_f (referred to the pseudo-fluorite cell) with the Y_2O_3 content.

where D is the crystallite size, λ is the wavelength of the radiation (1.4518 Å for Cu-K_α radiation), β is the corrected peak width at half-maximum intensity, and θ is the peak position. α-Al_2O_3 powder with a mean particle diameter of 25 μm was used to measure the instrumental broadening in order to correct the value of β. By using Equation 1 it was found that all powders had crystallite sizes in the range of 8–11 nm. A conjunct study of crystallite size and microstrain for all the powders will be presented below.

By applying the Rietveld method, it was found that all the powders have a tetragonal structure ($P4_2/nmc$ space group). The axial ratio c/a_f decreased with increasing Y_2O_3 content and became almost unity at 9 mol% Y_2O_3. However, powders in the compositional range of ZrO_2 - 9 to 12 mol% Y_2O_3 exhibited their oxygen atoms displaced from the ideal fluorite sites along the c axis. These results show that the t′/t″ limit is located around 9 mol% Y_2O_3, in accordance with the one reported by Yashima *et al.* [5–8]. The oxygen displacement was almost independent of the composition, with a value of (0.24 ± 0.01) Å for all the powders. Table II presents these results, while Figs 3 and 4 show the cell parameters for the pseudo-fluorite cell, a_f and c, and the axial ratio c/a_f, respectively.

The comparison between $P4_2/nmc$ and $Fm\bar{3}m$ for the ZrO_2 - 12 mol% Y_2O_3 powders is presented in Table III. It should be noted that the first model gives

TABLE II Structural parameters and standard Rietveld agreement factors obtained for the nanocrystalline ZrO_2 - 2.8 to 12 mol% Y_2O_3 powders. The axial ratio c/a_f is referred to the pseudo-fluorite cell

	2.8 mol% Y_2O_3	4 mol% Y_2O_3	5 mol% Y_2O_3	6 mol% Y_2O_3	7 mol% Y_2O_3
a (Å)	3.6067 (5)	3.6100 (5)	3.6162 (4)	3.6180 (5)	3.6251 (5)
c (Å)	5.1802 (6)	5.1647 (7)	5.1576 (6)	5.1438 (7)	5.1401 (8)
c/a_f	1.0156 (3)	1.0116 (3)	1.0085 (2)	1.0053 (3)	1.0026 (3)
z(O)	0.204 (1)	0.202 (1)	0.202 (1)	0.203 (1)	0.204 (1)
R_p	3.50	6.18	6.22	6.43	6.64
R_{wp}	4.54	8.12	8.08	8.37	8.63
R_{exp}	2.84	6.85	6.91	6.87	6.86
χ^2	2.56	1.40	1.36	1.48	1.58

	8 mol% Y_2O_3	9 mol% Y_2O_3	10 mol% Y_2O_3	11 mol% Y_2O_3	12 mol% Y_2O_3
a (Å)	3.6294 (4)	3.6286 (6)	3.6275 (6)	3.6297 (7)	3.6325 (9)
c (Å)	5.1433 (8)	5.1371 (8)	5.1371 (9)	5.1394 (10)	5.1426 (20)
c/a_f	1.0021 (3)	1.0011 (3)	1.0014 (3)	1.0012 (4)	1.0011 (7)
z(O)	0.204 (1)	0.202 (1)	0.204 (1)	0.202 (1)	0.205 (1)
R_p	6.85	6.16	6.01	6.21	5.77
R_{wp}	8.76	7.86	7.78	8.03	7.32
R_{exp}	7.06	5.86	5.79	5.90	4.47
χ^2	1.54	1.80	1.80	1.85	2.68

TABLE III Structural parameters and agreement factors obtained for the ZrO_2 - 12 mol% Y_2O_3 powders comparing the $P4_2/nmc$ and $Fm\bar{3}m$ models

	$P4_2/nmc$	$Fm\bar{3}m$
a (Å)	3.6325 (9)	5.1378 (14)
c (Å)	5.1426 (20)	
z(O)	0.205 (1)	
R_p	5.77	7.73
R_{wp}	7.32	9.20
R_{exp}	4.47	4.53
χ^2	2.68	4.13

TABLE IV Volume-weighted crystallite size ($\langle D\rangle_v$) and microstrain ($\tilde{e}$) values obtained for the nanocrystalline ZrO_2 - 2.8 to 12 mol% Y_2O_3 powders by employing the multiple-line integral breadth method

Y_2O_3 content	$\langle D\rangle_v$ (nm)	$\tilde{e}$ ($\times 10^{-3}$)
2.8 mol%	10.8 ± 0.3	3.2 ± 0.1
4 mol%	11.2 ± 0.3	4.4 ± 0.2
5 mol%	10.6 ± 0.3	4.8 ± 0.2
6 mol%	10.3 ± 0.3	5.2 ± 0.2
7 mol%	10.2 ± 0.3	5.3 ± 0.2
8 mol%	11.3 ± 0.3	4.9 ± 0.2
9 mol%	8.5 ± 0.2	4.9 ± 0.2
10 mol%	7.9 ± 0.2	4.9 ± 0.2
11 mol%	8.2 ± 0.2	5.2 ± 0.2
12 mol%	8.2 ± 0.2	4.5 ± 0.2

better agreement factors. As it has been emphasized in our previous work [15], these results are not in accordance with those reported by Yashima *et al.* [5–8], probably due to the small crystallite size obtained by the gel-combustion process.

For the size-strain analysis, the multiple-line integral breath method proposed by Langford *et al.* [26, 27] was employed by assuming a TCHZ-pV function for the line profile. Lorentzian and Gaussian components were considered for both crystallite size and microstrain broadening. The crystallite size profile presented both components, being the Lorentzian the more important one, as usually occurs [26–28]. On the contrary, the microstrain profile had a negligible Gaussian component, which is a surprising result since it is generally represented by a Gaussian function [26–28]. For example, this assumption is used in the single-line integral breadth method proposed by Keijser *et al.* [28].

Table IV shows the values of volume-weighted crystallite size ($\langle D\rangle_v$) and microstrain ($\tilde{e}$) for all the powders. The size-strain study showed that both contributions for the line broadening were appreciable, with values of $\langle D\rangle_v = 8$–11 nm (similar to those estimated by the Scherrer equation) and $\tilde{e} = 3$–5×10^{-3}. These values of $\tilde{e}$ are lower than those reported by J. D. Lin and J. Q. Duh for yttria- and ceria-doped zirconia powders synthesized by co-precipitation, which were of $\tilde{e} = 1$–2×10^{-2} [29, 30].

4. Conclusions

The tetragonal forms present in compositionally homogeneous, nanocrystalline ZrO_2 - 2.8 to 12 mol% Y_2O_3 powders have been studied by X-ray diffraction applying the Rietveld method. The t′/t″ boundary was at 9 mol% Y_2O_3, in accordance with previous works [5–8], but a larger t″ region was found (the t″/c boundary was reported to be at 11 mol% Y_2O_3). The t″/c boundary could not be determined.

A conjunct analysis of crystallite size and microstrain was carried out employing the multiple-line integral breath method and assuming Lorentzian and Gaussian component for both effects. A small Gaussian component was found, which was only due to crystallite size broadening. The values of the microstrain $\tilde{e}$ found in the present work were lower than those reported for powders synthesized by co-precipitation [29, 30].

Acknowledgements

The authors acknowledge Lic. R. E. Juárez and Lic. G. E. Lascalea for technical support.

References

1. S. P. S. BADWAL, *Solid State Ionics* **52** (1992) 23.
2. S. P. S. BADWAL and J. DRENNAN, in "Science of Ceramic Interfaces II," edited by J. Nowotny (Elsevier Science, Amsterdam, 1994) p. 71.
3. R. C. GARVIE, R. H. J. HANNINK and R.T. PASCOE, *Nature* **258** (1975) 703.
4. W. E LEE and W. M. RAINFORTH, "Ceramic Microstructures: Property Control by Processing" (Chapman & Hall, London, 1994) p. 317.
5. M. YASHIMA, K. OHTAKE, H. ARASHI, M. KAKIHANA and M. YOSHIMURA, *J. Appl. Phys.* **74** (1993) 7603.
6. M. YASHIMA, S. SASAKI, M. KAKIHANA, Y. YAMAGUCHI, H. ARASHI and M. YOSHIMURA, *Acta Cryst.* **B50** (1994) 663.
7. M. YASHIMA, M. KAKIHANA and M. YOSHIMURA, *Solid State Ionics* **86/88** (1996) 1131.
8. M. YASHIMA, K. OHTAKE, M. KAKIHANA, H. ARASHI and M. YOSHIMURA, *J. Phys. Chem. Solids* **57** (1996) 17.
9. M. YASHIMA, N. ISHIZAWA and M. YOSHIMURA, *J. Am. Ceram. Soc.* **76** (1993) 641.
10. *Idem., ibid.* **76** (1993) 649.
11. M. YASHIMA, K. MORIMOTO, N. ISHIZAWA and M. YOSHIMURA, *ibid.* **76** (1993) 1745.
12. M. YASHIMA, M. KAKIHANA, H. ARASHI and M. YOSHIMURA, *ibid.* **77** (1994) 1067.
13. M. YASHIMA, S. SASAKI, Y. YAMAGUCHI, M. KAKIHANA, M. YOSHIMURA and T. MORI, *Appl. Phys. Lett.* **72** (1998) 182.
14. M. YASHIMA, M. KAKIHANA, K. ISHII, Y. IKUMA and M. YOSHIMURA, *J. Mater. Res.* **11** (1996) 1410.
15. D. G. LAMAS and N. E. WALSÖE DE RECA, *Mater. Lett.* **41** (1999) 204.
16. L. A. CHICK, L. R. PEDERSON, G. D. MAUPIN, J. F. BATES, L. E. THOMAS and G. J. EXARTHOS, *ibid.* **10** (1990) 6.
17. L. R. PEDERSON, G. D. MAUPIN, W. J. WEBER, D. J. MCREADY and R. W. STEPHENS, *ibid.* **10** (1991) 437.
18. J. SCHÄFER, W. SIGMUND, S. ROY and F. ALDINGER, *J. Mater. Res.* **12** (1997) 2518.
19. S. T. ARUNA and K. C. PATIL, *NanoStruct. Mater.* **10** (1998) 955.
20. D. G. LAMAS, G. E. LASCALEA and N. E. WALSÖE DE RECA, *J. Eur. Ceram. Soc.* **18** (1998) 1217.
21. R. E. JUÁREZ, D. G. LAMAS, G. E. LASCALEA and N. E. WALSÖE DE RECA, *ibid.* **20** (2000) 133.
22. J. RODRÍGUEZ-CARVAJAL, Program FullProf. 98, version 0.2 (1998).
23. R. A. YOUNG, in "The Rietveld Method," edited by R. A. Young (International Union of Crystallography, Oxford University Press, Nueva York, 1995) p. 9.

24. H. G. SCOTT, *J. Mater. Sci*. **10** (1975) 1527.
25. H. KLUG and L. ALEXANDER, "X-ray Diffraction Procedures for Polycrystalline and Amorphous Materials" (John Wiley and Sons, New York, 1974) p. 618.
26. J. I. LANGFORD, R. DELHEZ, TH. H. DE KEIJSER and E. J. MITTEMEIJER, *Aust. J. Phys*. **41** (1988) 173.
27. R. DELHEZ, TH. H. DE KEIJSER, J. I. LANGFORD, D. LOUËR, E. J. MITTEMEIJER and E. SONNEVELD, in "The Rietveld Method," edited by R. A. Young (International Union of Crystallography, Oxford University Press, Nueva York, 1995) p. 132.
28. TH. H. DE KEIJSER, J. I. LANGFORD, E. J. MITTEMEIJER and A. B. P. VOGELS, *J. Appl. Cryst*. **15** (1982) 308.
29. J. D. LIN and J. Q. DUH, *J. Mater. Sci*. **32** (1997) 4901.
30. *Idem*., *ibid*. **32** (1997) 5779.

Received 11 November 1999
and accepted 2 March 2000